

Catalytic oxidative desulfurization of benzothiophene with hydrogen peroxide over Fe/AC in a biphasic model diesel-acetonitrile system

Guang-Jian Wang[†], Jian-Kang Zhang, and Ying Liu

School of Chemical Engineering, Qingdao University of Science and Technology, Qingdao 266042, Shandong, P. R. China
(Received 11 November 2012 • accepted 6 April 2013)

Abstract—Catalytic oxidative desulfurization (Cat-ODS) of benzothiophene (BT) in n-octane has been investigated with hydrogen peroxide (H₂O₂) over catalysts of activated carbon (AC) supported iron oxide under mild conditions. The catalyst was characterized by N₂ adsorption, XRD, SEM/EDS, TPR and XPS. Under the best operating condition for the catalytic oxidative desulfurization—temperature 60 °C, atmospheric pressure, 0.15 g Fe/AC, 18 molar ratio of hydrogen peroxide to sulfur, using acetonitrile as extraction solvent for double extraction—the sulfur content in model diesel fuel (MDF) was reduced from 700 ppmw to 30 ppmw with 95.66% of total sulfur was removed.

Key words: Activated Carbon, Catalytic Oxidative Desulfurization, Benzothiophene, Fe/AC Catalysts, Sulfur Removal

INTRODUCTION

Deep desulfurization of fuel oils has received increasing global attention due to the ever stringent sulfur content protocols. Diesel is widely used in the transport industry as the second major transportation fuel. However, a continual problem in using diesel fuel is of its high quantity of sulfur. Sulfur compounds in diesel fuel are converted to sulfur oxides (SO_x) during combustion, which not only contribute to acid rain and environmental pollution, but also cause inefficient performance of exhaust catalysts [1]. Although environmental regulation has been applied in many countries to reduce the sulfur levels (generally, less than 15 ppmw) in diesel and other fuels, sulfur removal still represents a major operational and economic challenge for the petroleum refining industry [2].

The current hydrodesulfurization (HDS) can efficiently remove reactive sulfides, disulfides, mercaptans and light thiophenic sulfur compounds, but it is less effective for refractory sulfur compounds, such as dibenzothiophene (DBT) and its derivatives with one or two alkyl groups, because of steric hindrance towards active sites in HDS catalysts. Moreover, this process requires high temperature (up to 400 °C), high hydrogen pressure (up to 100 atm), use of metal catalysts and large reactors, with long reaction time resulting in higher operational costs [3]. In this sense, to overcome the limitations of HDS, several alternative technologies, such as biodesulfurization [4], selective adsorption [5,6] and oxidative desulfurization [7-11], have been introduced to achieve ultra-low sulfur diesel fuel in recent decades.

Catalytic oxidative desulfurization (Cat-ODS) has been considered a promising method for deep desulfurization technology because it can be carried out under mild conditions, such as relatively low temperature, pressure and cost of operation when compared with HDS, and is capable to meet the future environmental regulation with low sulfur diesel or even sulfur-free diesel fuel [8]. Generally, Cat-ODS proceeds in two steps: oxidation of sulfur and followed by solvent

extraction or solid adsorbent. Hydrogen peroxide has been considered a powerful oxidant of sulfur compounds, and the best result will be achieved when using hydrogen peroxide in conjunction with heterogeneous catalysts. Various studies of catalytic oxidation system have been reported, such as H₂O₂/Mo/γ-Al₂O₃ [9], H₂O₂/Ti-HMS [10], H₂O₂/heteropolyanion [11] (phase transfer catalyst) and H₂O₂/activated carbon [12]. Under the ODS process, the sulfur compounds are oxidized to form highly polarized sulfoxides and sulfones. These sulfoxides and sulfones are substantially more polar than the respective sulfides, and then a solvent extraction step can be a convenient way to remove selectively the oxidized sulfur compounds from oil phase.

Iron species, including iron ions and iron oxides, have been extensively used for the catalytic decomposition of H₂O₂ in homogeneous and heterogeneous systems [13].



However, the homogeneous system has been gradually replaced by active heterogeneous processes in catalysis research due to the generation of large amounts of sludge caused by precipitation of ferric hydroxide, the necessity of operating at pH≈3, and the difficulty of catalyst recovery. The use of heterogeneous iron oxides overcomes these problems. The use of iron oxides as heterogeneous catalysts is possible over a wider pH range, including at neutral values, and physical sedimentation or magnetic separation can be used to separate the catalyst after completion of the reaction [14]. Recently, catalysts based on iron oxides dispersed over activated carbon have been successfully used in environmental applications [15]. Activated carbon has often been used as carrier due to its high surface area and rich surface chemistry. These interesting properties of activated carbon also allow the efficient dispersion of iron species throughout their porous structure [16].

As mentioned above, catalysts have been used in most investigations to enhance the efficiency of oxidant in ODS process. To the best of our knowledge, using Fe/AC as heterogeneous catalysts to oxidize sulfur-containing compounds in diesel has been rarely reported. Thus, according to the principle of Fenton or Fenton-like reaction systems, the catalyst Fe/AC was prepared and used in Cat-

[†]To whom correspondence should be addressed.
E-mail: wjnet@126.com

ODS process [17]. The objective of this work is to investigate catalytic oxidative desulfurization property using H_2O_2 as oxidant catalyzed by Fe/AC.

EXPERIMENTAL SECTION

1. Materials

Coconut shell activated carbons (20-50 mesh) were purchased from Fujian Xinsen Charcoal Industry Co., Ltd. $\text{Fe}(\text{NO}_3)_3 \cdot 9\text{H}_2\text{O}$, HNO_3 , and n-octane were used as analytical reagents and purchased from Beijing Chemical Reagent Co., Ltd. Benzothiophene was purchased from Japan Chemical Reagent Association Co., Ltd.

2. Catalyst Preparation

Activated carbons were washed by distilled water for several times with the aim of removing some ash and impurities. After that, deashed AC was dried in the air at 110°C for 12 h. The appropriate amount of AC was pretreated with $7.5 \text{ mol}\cdot\text{L}^{-1}$ HNO_3 at 90°C for 2 h, and then washed by distilled water until no further change of pH (around $\text{pH}=6$). Finally, the samples were then dried at 110°C for 12 h.

The preparation of all catalysts by incipient impregnation method was as follows. AC oxide with HNO_3 was used as catalyst support to impregnate with appropriate aqueous solution of $\text{Fe}(\text{NO}_3)_3 \cdot 9\text{H}_2\text{O}$. The well-impregnated samples were placed at room temperature for 2 h. Then the required amount of urea was slowly added to the samples, with thorough stirring at room temperature for 0.5 h. The mixed system was then heated at $90\text{--}95^\circ\text{C}$ and reacted for 2 h. Afterwards, the precipitates were separated from the solution by filtration, washed three times by deionized water and one time by anhydrous ethanol, and dried at 110°C overnight. Finally, the catalyst precursors obtained were calcined under the nitrogen atmosphere at different temperatures (300°C , 400°C , and 500°C) for 4 h in a tubular furnace producing the catalysts denoted as Fe/AC.

3. Catalyst Characterization

The catalysts were characterized by powder XRD analysis using a diffract meter (XRD, Rigaku D/MAX-2500/PC) with $\text{Cu K}\alpha$ radiation (1.540 \AA) in the 2θ range from 10° to 90° . The N_2 adsorption-desorption isotherms were measured using a Belsorp II system at -196°C . Prior to analysis, samples were evacuated at 150°C for 4 h. The Brunauer-Emmett-Teller (BET) surface area was calculated with the relative pressure ranging from 0.04 to 0.15. The total pore volume was derived from the amount adsorbed at the relative pressure of about 0.99. The pore size distributions were calculated by the Barrett-Joyner-Halenda (BJH) method according to the adsorption branches. Scanning electron microscopy (SEM) images were obtained using JEOL (JSM-7500F) with a secondary electron detector with energy dispersive X-ray spectroscopy (EDS). Temperature programmed reduction (TPR) experiments were carried out in a Auto-Chem 2920 instrument using 50 mg sample under $60 \text{ mL}\cdot\text{min}^{-1}$ H_2 (10%)/Ar with heating rate of $5^\circ\text{C}\cdot\text{min}^{-1}$. The XPS measurements were performed on an ESCALAB 250 (VG Scientific, U.K.) using a monochromated Al $\text{K}\alpha$ excitation source. The survey and high-resolution spectra were collected with 100 and 30 eV pass energies, respectively. Quantitative analysis was done with CASAXPS software after Shirley background subtraction.

4. Catalytic Tests

To do the catalytic oxidative desulfurization tests, model diesel

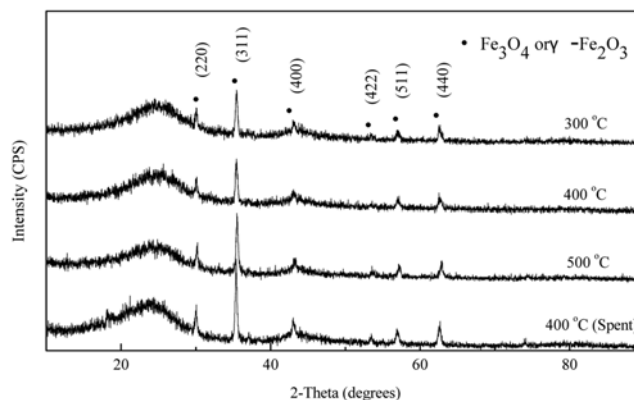


Fig. 1. XRD patterns of Fe/AC under different calcination temperatures.

fuel (MDF) was prepared by adding benzothiophene (BT) to liquid n-octane with the concentration of $0.0154 \text{ mol}\cdot\text{L}^{-1}$ (700 ppmwS). A typical experiment was performed as follows: In a 50 mL round-bottom flask equipped with a magnetic stirrer and a heated circulating bath, 10 mL of MDF was mixed with Fe/AC, and hydrogen peroxide 30 wt%, at 60°C and atmospheric pressure. The mixture was refluxed for 0.5-2 h under vigorous stirring at atmospheric pressure. After the reaction, the oxidized MDF was extracted by 10 mL acetonitrile, and the oil layers were collected and analyzed for sulfur content by gas chromatography with flame photometric detector (GC-FPD).

RESULTS AND DISCUSSION

1. Catalyst Characterization

To investigate the iron phases formed on the composites, XRD analyses were performed and the resulting patterns (Fig. 1) for all catalysts show relatively narrow bands and sharper diffraction peaks compared with previously reported. Diffraction peaks at $2\theta=30.2^\circ$, 35.5° , 43.1° , 53.5° , 57.0° and 62.6° related to the cubic iron oxide phases maghemite ($\gamma\text{-Fe}_2\text{O}_3$) and/or magnetite (Fe_3O_4), together with two broad bands, located at around 24.8° and $2\theta=44^\circ$ associated to the micrographitic structure characteristic of activated carbons, respectively [18]. As also can be seen from the XRD patterns, the sample calcined at 500°C shows slightly sharper diffraction peaks belonging to maghemite and/or magnetite than the XRD pattern of samples calcined at 300°C and 400°C , demonstrating that the crystalline phase grow with the increase of calcination temperature. Furthermore, XRD patterns for spent catalyst samples calcined at 400°C were also supplied to compare the changes of catalysts before and after Cat-ODS and ensure the catalyst phase and stability. As also can be seen from Fig. 1, no obvious changes of the catalyst phase were observed for the samples before and after Cat-ODS, demonstrating that the structure of catalyst was not destroyed and the catalyst showed higher stability.

The textural properties were investigated by nitrogen adsorption-desorption at -196°C (Fig. 2). The isotherms showed mainly microporous type features (Type I according to IUPAC classification) for all samples. The BET specific surface area (S_{BET}) and pore characteristics of the samples are listed in Table 1. As shown, calcination

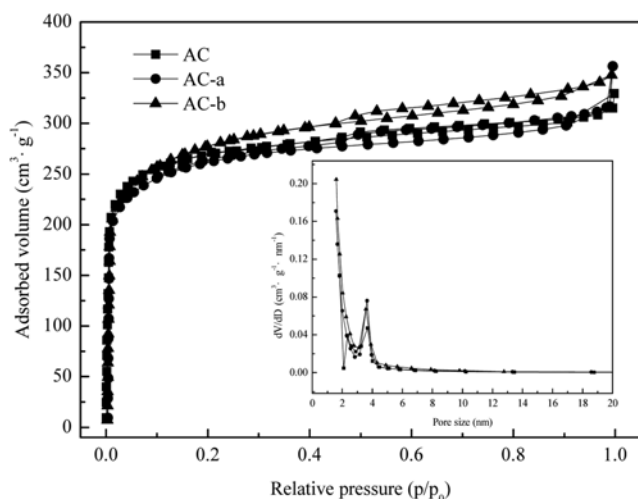


Fig. 2. The N_2 adsorption-desorption isotherms and pore size distributions (inset) of the materials.

Table 1. Specific surface area and pore structure parameters of the samples

Sample	S_{BET} (m^2/g)	S_{micro} (m^2/g)	V_t (cm^3/g)	V_{micro} (cm^3/g)	V_{micro}/V_t	D_p (nm)
AC	1001.1	556.8	0.5121	0.3609	0.70	2.05
AC-a	966.3	874.4	0.5539	0.3720	0.67	2.29
AC-b	1037.5	882.6	0.5343	0.3633	0.68	2.23
AC-c	1030.8	884.1	0.5406	0.3737	0.69	2.10
AC-d	1023.6	836.8	0.5512	0.3642	0.67	2.25

AC: non-modified activated carbon, AC-a: AC oxidized with 7.5 mol/L HNO_3 at 90 °C for 2 h, AC-b: catalysts of Fe/AC calcinated at 300 °C, AC-c: catalysts of Fe/AC calcinated at 400 °C, AC-d: catalysts of Fe/AC calcinated at 500 °C, D_p : average pore diameter

temperature on the effect of parameters of the sample is not obvious. Surface area and V_{micro}/V_t are slightly decreased compared with original activated carbon supports, but total pore volume is increased, which may correlate to the mild oxidation of 7.5 mol/L HNO_3 . Previous researches [19,20] have shown that pretreatment with HNO_3 can not only increase acidic oxygen-containing groups but also alter

the porous structure of AC surface, and those hydrophilic surface functional groups can also contribute to the dispersion of active components on the activated carbon carrier. Therefore, most activated carbon-based catalysts/adsorbents were nearly all pretreated with concerned HNO_3 , and we also take this process in preparing Fe/AC catalysts.

After iron impregnation, surface area and V_{micro}/V_t are slightly increased and no obvious changes were observed for total pore volume, which may correlate to the formation of iron oxide in activated carbon supports for iron oxide also has a relatively small surface area and pore volume. Moreover, the oxidation action of Fe(III) salt also plays a role as an activating agent for carbon materials [20]. In the case of the pore size distribution, two craters were observed for the original activated carbon, and the two craters shift to only one sharper crater after HNO_3 oxidation and impregnation of $Fe(NO_3)_3$ (shown in Fig. 2 (inset)); this may also relate to the activation effect of Fe(III) salt. Further investigations are needed to explain this phenomenon.

The morphological analyses were performed by SEM and are presented in Fig. 3. The SEM micrograph for AC (Fig. 3(a)) shows ordered and well developed pores which cover evenly the smooth surface. After iron impregnation, a similar morphology is observed. As can be seen from Fig. 3(b), the scattered white highlights are iron oxide particles which have been confirmed by using SEM/EDS, suggesting the formation of iron oxide particles well-dispersed covering the AC.

Characterization of EDS and XPS was further adopted to determine the loading content of Fe on the carbon nanosheets of the Fe/AC catalysts. The content of metals on the surface is listed in Table 2. As shown there, the values obtained using EDS and XPS are very close to the theoretical loadings. It is interesting that some deviations are observed between the two methods of analysis. EDS is typically a quick and simple method for characterization of carbon based catalysts, and with proper sample preparation and adequate data capture it can produce reliable results. The deviations here are attributed to the small sample size used for the EDS analysis. However, the values obtained by EDS analysis are not so much deviated from those determined by XPS analysis, which, in turn, demonstrates a good distribution and dispersion of iron oxides on the carbon support.

The obtained TPR profiles are displayed in Fig. 4. The first hy-

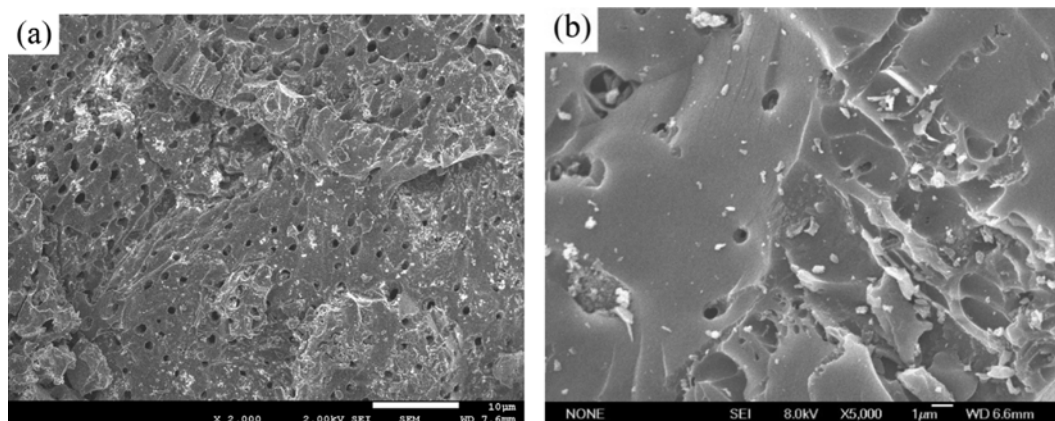
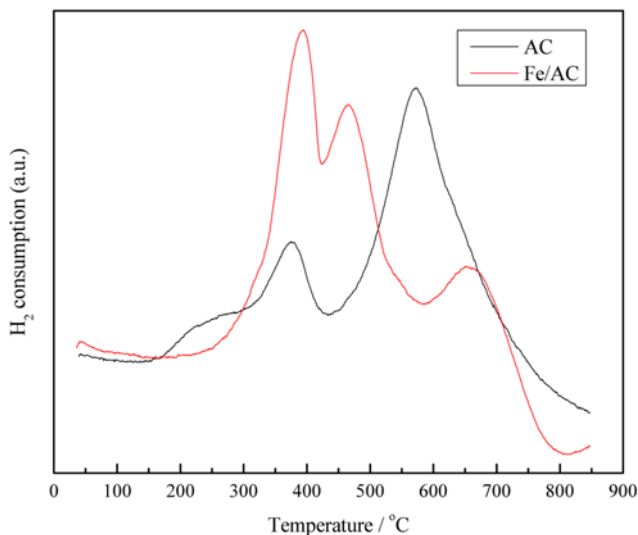


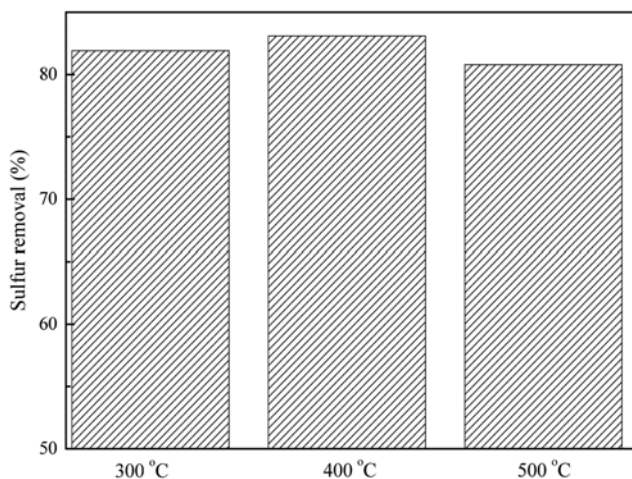
Fig. 3. Scanning electron micrographs of (a) AC and (b) Fe/AC.

Table 2. Contents of carbon, oxygen, and iron (at%) of Fe/AC catalysts

Test method	Iron content (%)	Carbon content (%)	Oxygen content (%)
EDS	2.51	81.72	15.77
XPS	3.28	84.14	12.58

**Fig. 4. H₂-TPR profiles of AC and Fe/AC (Calcined at 400 °C).**

drogen consumption peak appears at about 350 °C, which is attributed to the transformation of hematite to magnetite. The second hydrogen consumption peak appears at about 450 °C and this peak is attributed to the transformation of magnetite to wustite. The third hydrogen consumption peak seems broader than the other two, and this peak is correlated to the transformation of wustite to metallic iron. The three hydrogen consumption peaks correspond to the transformation the four phases of Eq. (2). The TPR profiles (Fig. 4) also show that the pure forms of activated carbon (oxidized with 7.5 mol/

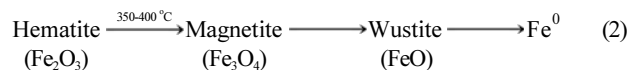
**Fig. 5. Sulfur removal rate of catalysts under different calcination temperatures. Conditions: $C_{catalyst}=10 \text{ g}\cdot\text{L}^{-1}$, $T=60 \text{ }^\circ\text{C}$, $\text{H}_2\text{O}_2/\text{S}=8:1$ (molar ratio) and $t=30 \text{ min}$.**

L HNO_3) can react with hydrogen when the temperature is approximately 300 °C, and hydrogen consumption increases sharply with an intense peak around 600 °C, which is an already known property of activated carbon due to its rich surface chemistry [21].

2. Catalytic Evaluation

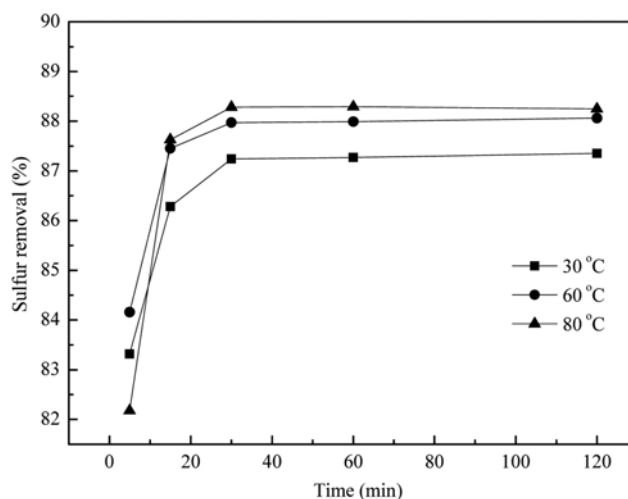
2-1. Effect of Calcination Temperature on Sulfur Removal

As can be seen from Fig. 5, there is no obvious difference of desulfurization performance for the catalysts due to the fact that both maghemite ($\gamma\text{-Fe}_2\text{O}_3$) and magnetite (Fe_3O_4) can promote hydrogen peroxide decomposition to hydroxyl radicals capable to efficiently oxidize BT. On one hand, lower calcination temperature (300 °C) may lead to leaching of active component due to the weak binding force between carrier and active component [22], and higher calcination temperature (above 500 °C) will contribute to crystal phase transition of active component (Eq. (2)). Calcination temperatures and calcination time may influence the BET surface area and crystallinity of catalyst, and further influence the decomposition of H_2O_2 and sulfur removal. Thus further study is needed to investigate the effect of calcination temperatures and calcination time in the following work. In view of the color of samples, red-brown particles can be observed for the samples calcined at 300 °C and 400 °C, which contributes to the formation of Fe_2O_3 . However, there only black particles can be observed when calcined at 500 °C, which correlates with the formation of Fe_3O_4 . This phenomenon shows that the active component changed from red-brown Fe_2O_3 to black Fe_3O_4 with the increase of calcination temperature from 300 °C to 500 °C. On the other hand, the results showed that sample calcined at 400 °C had the highest sulfur removal rate (83.09%); thus the best calcination temperature was set at 400 °C.



2-2. Effect of Reaction Temperatures on Sulfur Removal

This experiment is conducted with the aim to investigate the effect of the temperature on the process of sulfur removal under catalytic oxidation and to determine the appropriate temperature and time. Fig. 6 shows the efficiency of desulfurization in the Cat-ODS

**Fig. 6. Effect of temperatures on Cat-ODS. Conditions: $C_{catalyst}=10 \text{ g}\cdot\text{L}^{-1}$ and $\text{H}_2\text{O}_2/\text{S}=10:1$ (molar ratio).**

reaction versus the reaction time at three different temperatures (30 °C, 60 °C and 80 °C). It indicates that the reaction temperature plays a very important role in the oxidative reaction. Although an increase in the reaction temperature from 30 °C to 80 °C led to an increase in the reaction rate and desulfurization performance, oxidation at higher temperature was unfavorable due to the decomposition of hydrogen peroxide to undesirable side products (H₂O and O₂) other than hydroxyl radicals, which decreases the efficiency of the desulfurization process and affects the quality of diesel fuel [23]. Moreover, reaction at temperature higher than 80 °C may lead to the oxidation of useful components in the fuel. In view of these results, the reaction temperature employed for Cat-ODS was set at 60 °C. Longer reaction duration for oxidative desulfurization will yield more complete oxidation of organosulfur compounds to their corresponding sulfones. However, no obvious sulfur removal rate changes were observed when the reaction time was more than 30 min; thus the best reaction time employed for Cat-ODS was set at 30 min.

2-3. Effect of H₂O₂/S Molar Ratios on Sulfur Removal

To investigate the effect of the concentration of the H₂O₂ oxidant on the sulfur elimination, the oxidation of BT with various H₂O₂/S molar ratios was carried out at 60 °C. From the results in Fig. 7, the H₂O₂/S molar ratio has a strong influence on the sulfur removal rate. The removal of BT was promoted with the increase of the H₂O₂/S molar ratio. Sulfur removal rate was only 25.49% when the H₂O₂/S molar ratio was 0. In this case, the removal of BT was only by means of adsorptive effect of Fe/AC. The sulfur removal rate in 30 min increased from 80.86% at H₂O₂/S=3 to 85.16% at H₂O₂/S=18. With the further increase of the H₂O₂/S ratio, the sulfur removal rate was reduced. This decrease could be explained probably by the excessive nonproductive decomposition of hydrogen peroxide to oxygen and water when H₂O₂ concentration was higher than a certain value (Scheme 1). This result was in agreement with a study conducted by Duarte et al. [7], who reported that higher values of molar proportion led to the reduction of sulfur removal rate. Therefore, H₂O₂/S=18 was chosen as the best molar ratio.

According to previous studies [24], the hydrogen peroxide was reacting according to two reaction pathways, an oxidation pathway

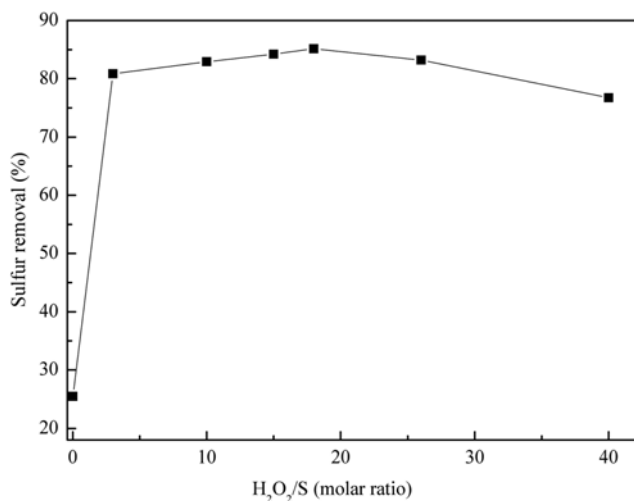
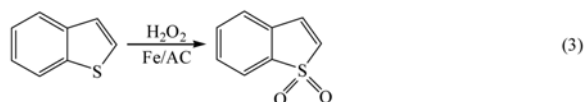
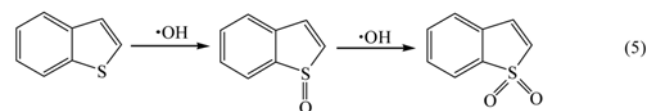


Fig. 7. Effect of different H₂O₂/S molar ratios on Cat-ODS. Conditions: $C_{catalyst} = 10 \text{ g} \cdot \text{L}^{-1}$, $T = 60 \text{ }^\circ\text{C}$ and $t = 30 \text{ min}$.

Over all reaction



Pathway 1:



Pathway 2:



Scheme 1. Cat-ODS reaction between oxidant and BT.

and a decomposition pathway, as shown in Scheme 1. The oxidation pathway proceeds via radicals attack on BT to form its corresponding sulfone. In pathway 1, hydrogen peroxide is decomposed by Fe/AC to generate hydroxyl radicals ($\cdot\text{OH}$). Hydroxyl radicals are very strong oxidants, and the oxidation electrode potential is up to 2.80 V, which is powerful enough for oxidation of BT [25]. On the other hand, the oxidative activity of hydrogen peroxide in Cat-ODS process was inhibited and influenced by a competitive pathway, which involved the decomposition of hydrogen peroxide to oxygen and water as shown in pathway 2. That is, not all the hydrogen peroxide introduced was utilized in situ formation of hydroxyl radicals used for oxidation of BT.

2-4. Catalyst Dosage on Sulfur Removal

Fig. 8 presents the dosage of Fe/AC loading into Cat-ODS process. The results obtained revealed that the optimum dosage of catalyst was $15 \text{ g} \cdot \text{L}^{-1}$ of MDF. Thus, in this Cat-ODS process, 0.15 g of the activated carbon was required to catalyze the oxidative desulfurization of 10 mL of MDF. As also can be seen from Fig. 7, the sulfur removal rate in the reaction system without Fe/AC was 71.74%, which was much lower than the system containing Fe/AC (84.56%). This result is in agreement with the study conducted by

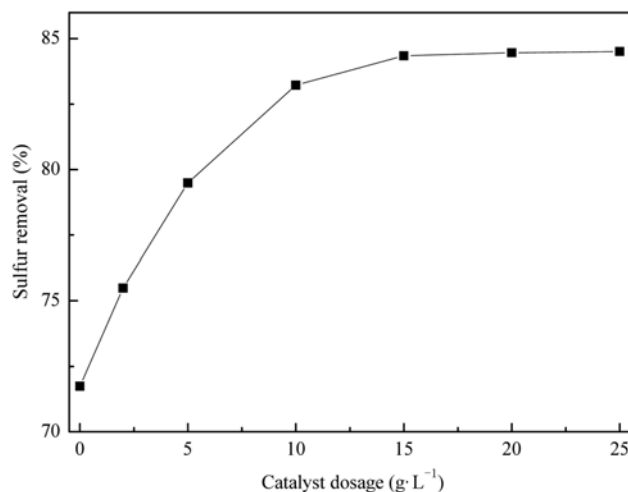


Fig. 8. Effect of different catalyst dosage on Cat-ODS. Conditions: H₂O₂/S=10 : 1 (molar ratio), $T = 60 \text{ }^\circ\text{C}$ and $t = 30 \text{ min}$.

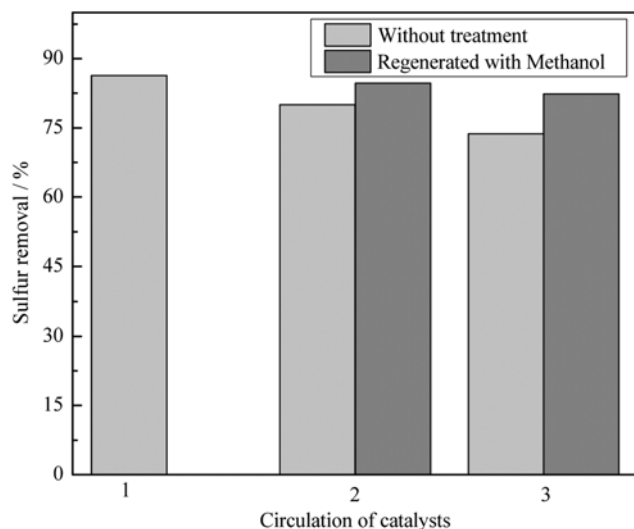


Fig. 9. The catalysts repeated use performance on Cat-ODS. Conditions: $C_{catalyst}=10\text{ g}\cdot\text{L}^{-1}$, $\text{H}_2\text{O}_2/\text{S}=18:1$ (molar ratio), $T=60\text{ }^\circ\text{C}$ and $t=30\text{ min}$.

Riad and his coworkers [26], who reported that only 22.7% of sulfur removal was achieved in the reaction without the presence of catalyst. This indicated that the presence of Fe/AC can significantly improve the efficiency of the reaction system with an increment of 12.82%, and this may also correlated to the good adsorptive property of Fe/AC. As is known, activated carbon based materials are usually used as adsorbent due to their high adsorption surface and developed porosity. Castro and coworkers [16], who studied the removal of the methylene blue (MB) model from aqueous solution, concluded the intense removal of the model was through combination of adsorption and oxidation processes. It is believed that the prepared Fe/AC can act both as a catalyst and an adsorbent in this Cat-ODS process.

2-5. The Catalysts Repeated Use Performance on Sulfur Removal

Fig. 9 shows the catalysts repeated use performance on Cat-ODS. The used catalysts were recovered, regenerated by solvent extraction in order to remove the adsorbed species and then dried at $110\text{ }^\circ\text{C}$ for 12 h. For comparison, the repeated use performance using catalysts without any treating was also conducted. As can be seen from Fig. 8, sulfur removal decreased from 86.37% to 73.74% after triple use of catalysts without solvent treatment, and sulfur removal still reached 82.34% using the catalysts regenerated by methanol. The results show that deactivation of catalysts can be inhibited by methanol extraction to remove the adsorbed species (BT/BTO_2) on the surface Fe/AC catalysts, suggesting that the catalysts regenerated by methanol have a better repeated use performance. Moreover, the catalysts of Fe/AC can be easily recovered after completion of the reaction by means of physical sedimentation or magnetic separation, which provides a good precondition for the repeated use of the catalysts.

2-6. Repetition Extraction on Sulfur Removal

According to previous studies [10-12] organosulfur compounds are generally polar and an extraction step is necessary to remove sulfur compounds, mainly in their oxidized form. As a general requirement, the solvent must have high polarity and to be insoluble in the oil. Based on previous work using Cat-ODS procedure [7], extrac-

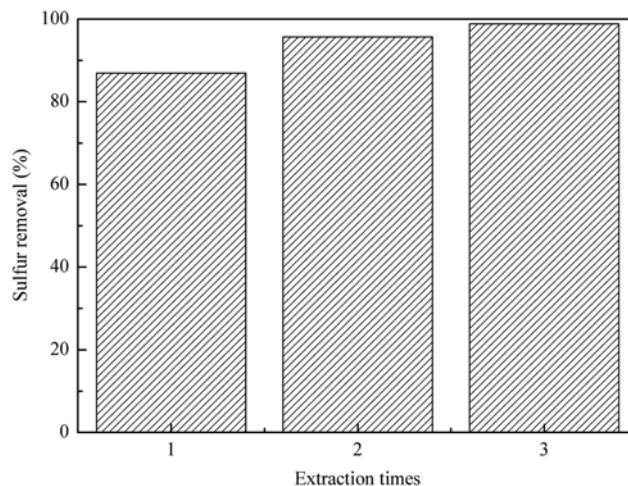


Fig. 10. Effect of repetition extraction on Cat-ODS. Conditions: $C_{catalyst}=10\text{ g}\cdot\text{L}^{-1}$, $\text{H}_2\text{O}_2/\text{S}=18:1$ (molar ratio), $T=60\text{ }^\circ\text{C}$ and $t=30\text{ min}$.

tion times using acetonitrile as extractant were also investigated in order to further improve the sulfur removal. The sulfur removal in 30 min increased from 86.95% at single extraction to 95.66% at double extraction. However, with the further increase of the extraction times (triple extraction), the increase of the removal became not obvious and the recovery of oil might be decreased [20]. What's more, solvent consumption is also needed to be considered in view of the experimental cost. Thus, double extraction was adopted after Cat-ODS reaction.

CONCLUSIONS

Activated carbon loaded iron oxide as catalysts exhibited high catalytic activity in Cat-ODS with H_2O_2 as oxidant. The active component was maghemite and magnetite, and catalysts showed best desulfurization performance when calcinated at $400\text{ }^\circ\text{C}$.

After the catalytic oxidative treatment, MDF containing 700 ppmw sulfur was successfully reduced to 30 ppmw of sulfur by using the H_2O_2 -Fe/AC system (95.66% of total sulfur removal). The catalysts of Fe/AC can be easily recovered by simple physical sedimentation or magnetic separation, and sulfur removal still reached 82.34% after triple use of catalysts regenerated by methanol. These results may indicate that Fe/AC has the potential to be used as catalyst in Cat-ODS to meet the future regulation of sulfur in diesel fuels.

ACKNOWLEDGEMENTS

We gratefully acknowledge the research grants provided by the National Natural Science Foundation of China (21076110).

REFERENCES

1. V. C. Srivastava, *RSC Adv.*, **2**, 759 (2012).
2. B. Pawelec, R. M. Navarro, J. M. Campos-Martin and J. L. G. Fierro, *Catal. Sci. Technol.*, **1**, 23 (2011).
3. X. L. Ma, L. Sun and C. S. Song, *Catal. Today*, **77**, 107 (2002).
4. N. Gupta, P. K. Roychoudhury and J. K. Deb, *Appl. Microbiol. Bio-*

- technol.*, **66**, 356 (2005).
5. X. L. Tang, W. Qian, A. Hu, Y. M. Zhao, N. N. Fei and L. Shi, *Ind. Eng. Chem. Res.*, **50**, 9363 (2011).
 6. K. S. Kim, S. H. Park, K. T. Park, B. H. Chun and S. H. Kim, *Korean J. Chem. Eng.*, **27**, 624 (2010).
 7. F. A. Duarte, P. A. Mello and C. A. Bizzi, *Fuel*, **90**, 2158 (2011).
 8. K. G. Hawa, W. Azelee and W. A. Bakar, *Fuel Process. Technol.*, **91**, 1105 (2010).
 9. Y. H. Jia, G. Li and G. L. Nin, *Fuel Process. Technol.*, **92**, 106 (2011).
 10. Y. Wang, G. Li, X. S. Wang and C. Z. Jin, *Energy Fuels*, **21**, 1415 (2007).
 11. K. Yazu, Y. Yamamoto, T. Furuya, K. Miki and K. Ukegawa, *Energy Fuels*, **15**, 1535 (2001).
 12. G. X. Yu, S. X. Lu, H. Chen and Z. N. Zhu, *Carbon*, **43**, 2285 (2005).
 13. J. H. Ramirez, F. J. Maldonado-Hodar, A. F. Perez-Cadenas, C. Moreno-Castilla, C. A. Costa and L. M. Madeira, *Appl. Catal. B-Environ.*, **75**, 312 (2007).
 14. A. Dhakshinamoorthy, S. Navalon, M. Alvaro and H. GarciaMetal, *Chem. Sus. Chem.*, **5**, 46 (2012).
 15. C. S. Castro, L. C. A. Oliveira and M. C. Guerreiro, *Catal. Lett.*, **133**, 41 (2009).
 16. C. S. Castro, M. C. Guerreiro, L. C. A. Oliveira, M. Gonçalves, A. S. Anastácio and M. Nazzarro, *Appl. Catal. A-Gen.*, **367**, 53 (2009).
 17. F. Duarte, F. J. Maldonado-Hodar, A. F. Perez-Cadenas and L. M. Madeira, *Appl. Catal. B-Environ.*, **85**, 139 (2009).
 18. M. A. Fontecha-Camara, M. A. Alvarez-Merino and F. Carrasco-Marin, *Appl. Catal. B-Environ.*, **101**, 425 (2011).
 19. Y. F. Jia and K. M. Thomas, *Langmuir*, **16**, 1114 (2000).
 20. M. H. Do, N. H. Phan, T. D. Nguyen, T. T. Suong Pham, V. K. Nguyen, T. T. Trang Vu and T. D. Nguyen, *Chemosphere*, **85**, 1269 (2011).
 21. L. C. A. Oliveira, N. S. Cristina, M. I. Yoshida and M. L. Rochel, *Carbon*, **42**, 2279 (2004).
 22. R. M. Liou and S. H. Chen, *J. Hazard. Mater.*, **172**, 498 (2009).
 23. Z. Wu and B. Ondruschka, *Ultrason. Sonochem.*, **17**, 1027 (2010).
 24. I. R. Guimaraes, A. Giroto, L. C. A. Oliveira, M. C. Guerreiro and D. Q. Lima and J. D. Fabris, *Appl. Catal. B-Environ.*, **91**, 581 (2009).
 25. B. R. Petigara, N. V. Blough and A. C. Mignerey, *Environ. Sci. Technol.*, **36**, 639 (2002).
 26. M. Riad and S. Mikhail, *Catal. Sci. Technol.*, **2**, 1437 (2012).